

Highly Concentrated $\text{Si}_{1-x}\text{C}_x$ Alloy with an Ordered Superstructure

Weiping Qin, Changfeng Wu, Guanshi Qin, Jisen Zhang, and Dan Zhao

*Key Laboratory of Excited State Processes, Changchun Institute of Optics, Fine Mechanics and Physics,
Chinese Academy of Sciences, Changchun 130022, China*

(Received 23 March 2003; published 19 June 2003)

An ordered Si-C alloy was observed in the products resulting from thermal reduction of molybdenum disilicide heating rods. High-resolution transmission electron microscopy measurements indicate that the $\text{Si}_{1-x}\text{C}_x$ alloy with $x \approx 25\%$ is pure, single crystalline, and possesses a superlattice structure. The superlattice periodicity occurs along the diamond [001] direction and corresponds to the quintupling of the primary (002) periodicity. The possible growth mechanism is discussed. The Mo element is likely to play a crucial role in the growth process of the $\text{Si}_{1-x}\text{C}_x$ alloy, since it can both reduce the energy required for breaking up C clusters and contribute to surface modification, which are of great benefit to enhance the carbon concentration and induce an ordered structure.

DOI: 10.1103/PhysRevLett.90.245503

PACS numbers: 61.66.Dk, 68.35.Dv, 68.37.Lp, 81.05.Bx

Group-IV semiconductor alloys have attracted much attention recently because they offer numerous practical applications in both microelectronics and integrated optoelectronic devices. Incorporation of carbon into silicon lattice represents a promising method for band gap engineering. However, the equilibrium solubility of C in Si is very small (3×10^{17} atoms/cm³) due to the large difference in covalent radii between the two elements. So there exists a great challenge to the growth of $\text{Si}_{1-x}\text{C}_x$ alloys with high C concentrations. Recent experimental efforts to overcome this obstacle are based on nonequilibrium methods, such as molecular beam epitaxy, which exploit the less constrained environment and the higher atomic mobility on surfaces [1]. Even when the nonequilibrium methods are used, only small amounts of carbon (a few percent) can be introduced without giving rise to SiC precipitation [2]. Alternative ways using precursor chemistry and ultrahigh-vacuum chemical vapor deposition were developed to create highly concentrated films ($\text{C} > 4$ at. %) that are inaccessible by conventional routes [3,4]. At present, these artificial thin alloy films, which exhibit certain desired characteristics such as improved mechanical stability and tailored electronic properties, are being vigorously pursued for a wide range of technological applications.

On the other hand, some basic issues in elemental semiconductor alloys, for instance order-disorder transitions, are also fascinating from a purely scientific viewpoint. Ordering in the $\text{Si}_{1-x}\text{Ge}_x$ alloy was first observed by Ourmazd and Bean [5]. Subsequently, several theoretical studies have tried to explain the ordering on the basis of the energetics and thermodynamics of the bulk Si-Ge alloy [6–8]. Later, LeGoues *et al.* demonstrated that it is an entirely kinetic phenomenon governed completely by growth conditions and surface reconstructions, and not by bulk thermodynamic equilibrium [9–11]. While experiments and theoretical studies combined together have led to important progress in the

general understanding of long-range order in the Si-Ge system, an open question still remains. How about the Si-C system?

Here, we report on an ordered Si-C phase with a considerably high C concentration produced by a thermal reduction of molybdenum disilicide (MoSi_2) heating rods. Energy-dispersive x-ray (EDX) spectroscopy has shown the composition of the material to be $\text{Si}_{1-x}\text{C}_x$ with $x \approx 25\%$. Using electron diffraction and high-resolution electron microscopy, an ordered superlattice structure has been identified in the alloy.

Our synthesis is based on thermal evaporation of MoSi_2 rods under controlled temperature and atmosphere. An ordinary electric furnace equipped with MoSi_2 rods was used as the heating device. A 20 ml alumina crucible filled with ammonium hydrogen difluoride ($\text{NH}_4\text{F} \cdot \text{HF}$) was placed at the center of the furnace where the temperature was kept at 650 °C and the pressure was under a normal atmospheric pressure. At this temperature, $\text{NH}_4\text{F} \cdot \text{HF}$ was decomposed into N_2 , H_2 , and HF gases, the two active components of which generated a reducing atmosphere in the furnace, resulting in the evaporation of MoSi_2 heating rods. During the evaporation, some thin films formed on the heating rods. After 2 h, these thin films were quickly taken out of the furnace. The obtained products were mainly characterized by a high-resolution transmission electron microscopy (HRTEM, JEOL 2010 at 200 kV operating voltage, equipped with energy-dispersive detection of the x rays emitted by an area of about $\pi \times 2^2$ nm² of the sample).

Thermal reduction of the MoSi_2 rods resulted in transparent colorless filmlike products that formed in high yield on the heating rod surface. TEM observations revealed that the products consist of a large quantity of nanowires and nanocables of silicon and silicides. In this Letter, we focus our attention on a new Si-C phase appearing in the products and its basic structural properties. Figure 1(a) shows a TEM image of the Si-C phase. The

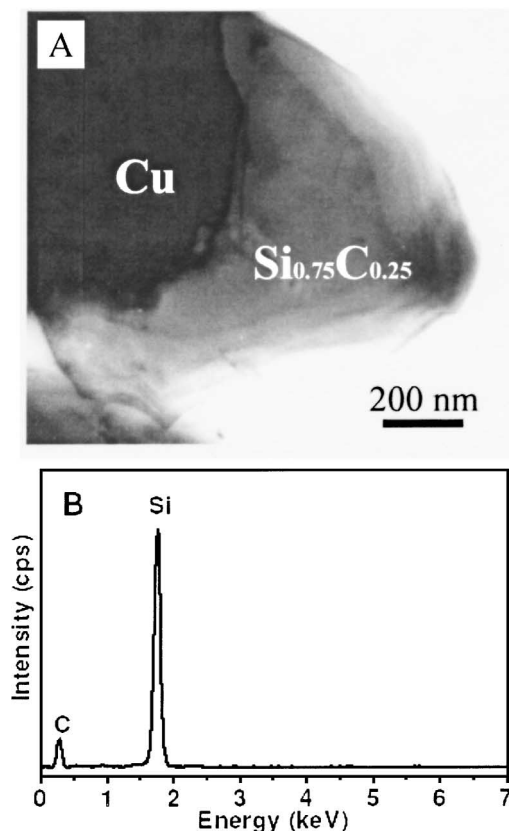


FIG. 1. Morphology and composition of the $\text{Si}_{1-x}\text{C}_x$ alloy. (a) TEM image of the $\text{Si}_{1-x}\text{C}_x$ alloy produced by simply evaporating MoSi_2 rods. The material was embedded in copper for ion-beam milling to prepare the specimen for TEM observations. Copper appears darker in diffraction contrast than the $\text{Si}_{1-x}\text{C}_x$ alloy. (b) EDX spectrum recorded from the alloy. The composition was calculated to be $\text{Si}_{0.75}\text{C}_{0.25}$ and kept constant throughout the material.

darker area in diffraction contrast (upper-left side) derives from copper in which the $\text{Si}_{1-x}\text{C}_x$ material was embedded for ion-beam milling during preparation of the specimen for TEM observations. EDX fluorescence analysis revealed that the sample contains only silicon and carbon, as indicated in Fig. 1(b). Quantitative analyses of the EDX spectra showed that the atomic composition ratio of Si/C is 3:1. The value keeps constant throughout the sample, indicating that the carbon is uniformly distributed in the material. In fact, $\text{NH}_4\text{F} \cdot \text{HF}$ and MoSi_2 do not contain a carbon element. Presumably, this unintentional impurity stems from a silicon carbide rod with one end contacting with a MoSi_2 rod in the furnace and the other end serving as an outer electrode.

A convergent beam electron diffraction pattern (Fig. 2) indicates that the $\text{Si}_{1-x}\text{C}_x$ alloy is single crystalline and has a cubic structure with Si and C atoms residing on sites of the diamond crystal structure. The diffraction pattern could be indexed for the $[110]$ zone axis and consists of the primary diamond cubic spots as well as four additional superlattice spots between (000) and (002) primary

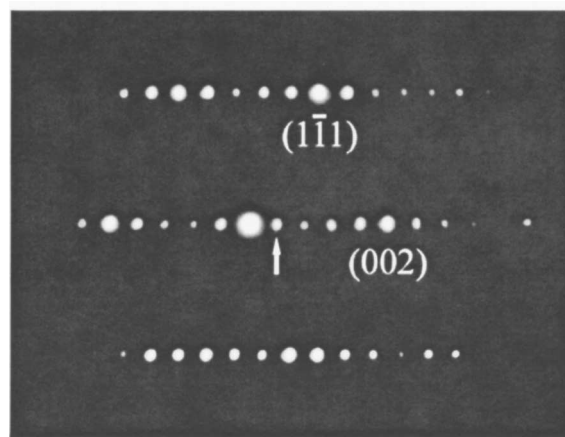


FIG. 2. Convergent beam electron diffraction pattern recorded along the $[110]$ zone axis. Additional weak spots between (000) and (002) primary spots correspond to the quintupling of the (002) periodicity. Note that the (002) reflection is due to double diffraction of the diamond cubic lattice.

spots. The additional weak spots, one of which was marked by an arrow, correspond to the quintupling of the (002) periodicity, suggesting the formation of an ordered superstructure.

High-resolution electron micrograph [Fig. 3(a)] provides further insight into the structure of the material. HRTEM shows that the $\text{Si}_{1-x}\text{C}_x$ alloy is structurally uniform and no obvious defects such as twins and stacking faults are observed. By analyzing the diffraction pattern and the HRTEM image, the average lattice parameter of the diamond cubic cell was determined to be 0.48 nm, a little smaller than the lattice parameter of Si ($a_{\text{Si}} = 0.54$ nm). The variance of the lattice constants is due to the extreme difference between the native bond lengths of the constituents, which are 0.24 nm for Si and 0.16 nm for diamond. The reduction in the lattice parameter with C incorporation suggests that the C impurities prefer the substitutional rather than the interstitial sites in the silicon lattice, which is consistent with the results of the lowly concentrated $\text{Si}_{1-x}\text{C}_x$ alloy [12,13]. A digital diffractogram, based on the Fourier transform of the experimental image, was used to produce the simulated image [Fig. 3(b)] that clearly confirmed the expected superstructure. The superlattice periodicity occurs along the $[001]$ direction and is 5 times larger than the lattice spacing of the primary (002) plane. Detailed HRTEM observations indicate that the whole sample shown in Fig. 1(a) possesses this ordered superstructure.

The high carbon concentration is obviously an important factor in the formation of this new phase since similar ordering has not been reported in lowly concentrated $\text{Si}_{1-x}\text{C}_x$ alloys. It is reasonable to conjecture that a silicon seed nucleates at the initial stage, and then there

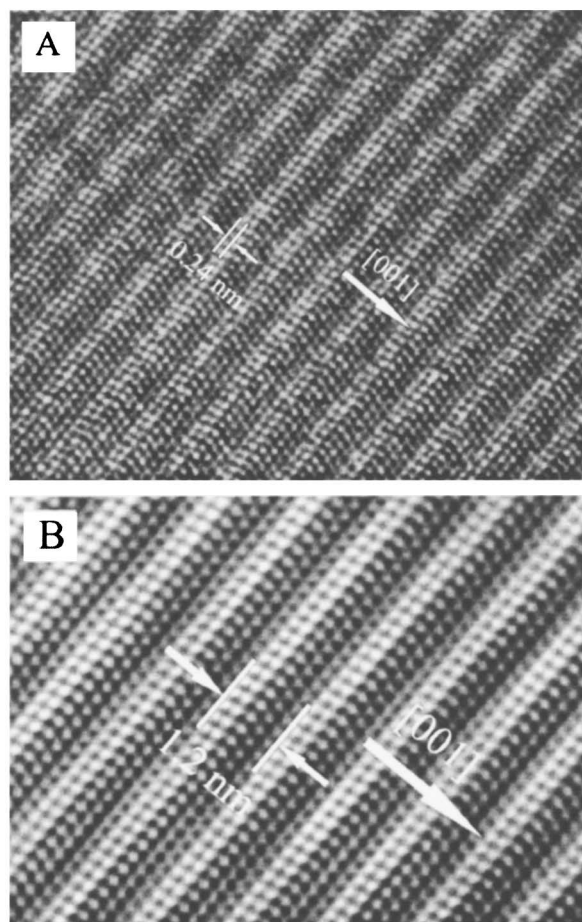


FIG. 3. High-resolution electron micrograph and simulated image of the $\text{Si}_{1-x}\text{C}_x$ alloy. (a) HRTEM image of the $\text{Si}_{1-x}\text{C}_x$ superstructure, showing a uniform structure and no obvious defect. (b) Simulated image of the ordered structure, obtained from a digital diffractogram based on the Fourier transform of the experimental image.

exists a Si growing surface, around which the Si, C, and Mo species aggregate due to the decomposition of the heating rods. To find out the reason for such a high C concentration residing in the material, the role of the Mo component should be considered since many transition metals, including Mo [14], can be used as catalysts to direct the growth of low-dimensional structures. It is generally accepted that C forms small clusters [15], and these clusters do not diffuse as easily as atomic species on or into the Si surface. More recently, Tsui and Ryan [16] demonstrated that the Mo as a catalyst can significantly reduce the energy required for breaking up C clusters, which has been predicted to cost several eV, particularly for small clusters. Moreover, in an important contribution to this problem, Tersoff [17] showed that the presence of the surface and the surface reconstruction can significantly enhance the solubility and diffusion of C atoms near the surface. The factors mentioned above may lead to a dramatic enhancement of C solubility in the subsurface

layers, which are in equilibrium with the surface. Diffusion is known to be rapid near the surface and negligibly slow in the bulk. Consequently, under typical growth conditions the carbon-enriched layers near the surface will be buried by further growth, permitting the formation of the highly concentrated alloy.

Kesan *et al.* [11] demonstrated that long-range order in $\text{Si}_{1-x}\text{Ge}_x$ occurs due to local segregation induced by the reconstruction strain field at the growing surface. According to this mechanism, the same “bulk” ordering as in $\text{Si}_{1-x}\text{Ge}_x$ should be observed in the $\text{Si}_{1-x}\text{C}_x$ alloy, as predicted by Tersoff [17]. Figure 4 shows a side view of the Si(100) 2×1 surface structure. The first, second, third, fourth, and fifth layers near the surface are labeled by 1, 2, 3, 4, and 5, respectively. Surface dimers are on the top, as indicated by yellow spheres. According to theoretical calculations [2,18], the second layer (blue spheres) and the fifth layer (violet spheres) were considered to be energetically unfavorable for C incorporation, while the third and fourth layer sites have much lower energy. Because of the surface reconstruction, the sites below the dimers (α sites, corresponding to red spheres) are under compressive stress, while the sites between the dimers (β sites, green spheres) are under tensile stress. For the Si-Ge system, the atomic-scale stresses can cause site-specific segregation of Si and Ge atoms, since the sites under compressive stress would rather be occupied by the smaller Si atom while those under tensile stress would be favored by the larger Ge atom. This segregation, once established on the surface, is essentially frozen into the bulk, resulting in an ordered $\text{Si}_{1-x}\text{Ge}_x$ alloy. However, in the Si-C case, no long-range order has been observed

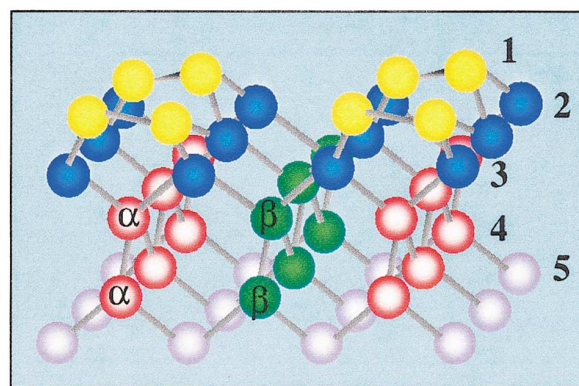


FIG. 4 (color). Side view of the Si(100) 2×1 reconstructed surface. The numbers 1–5 denote the first, second, third, fourth, and fifth layers near the surface, respectively. Surface dimers are at the top, as indicated by the yellow spheres. The α sites corresponding to red spheres are under compressive stress, while the β sites corresponding to green spheres are under tensile stress. The second layer (blue spheres) and the fifth layer (violet spheres) were considered to be energetically unfavorable for C incorporation, while the third and fourth layer sites have much lower energy [2,18].

in experiments before this paper. Kelires *et al.* [19] suggested that the stress-driven mechanism, disregarding the repulsive interaction between C atoms, needs modification for a high concentration alloy, although it works well when the interaction among the solute atoms is attractive or at least neutral (as in $\text{Si}_{1-x}\text{Ge}_x$). Rücker *et al.* [20] proposed that in bulk Si certain structures where the C atoms are arranged as third-nearest neighbors are more stable than isolated C impurities. Experimental studies and theoretical calculations are both varying in the preference between surface and subsurface sites. The exact location of the incorporated C atoms is still under debate. More recently, Remediakis and co-workers [1] revealed theoretically that an ordered third-layer C configuration could induce an ordering behavior in the distribution of subsurface C atoms. Kim *et al.* [18] demonstrated that the presence of C atoms in the Si(100) surface leads to a surface modification. Because of the surface modification, all the C atoms prefer to occupy the fourth layer α site at the initial stage of the C incorporation and the embedded carbon displays a one-dimensional ordering. In our growth conditions, the presence of Mo atoms contributes further to the surface modification, as previously observed by Bedrossian [21,22]. The surface modification would result in the concurrent change of the most stable C incorporation sites and the redistribution of the C content in subsurface layers. The Mo-modified Si surface is likely to serve as a template which induces that Si and C atoms arrange themselves into the energetically stable sites, forming an ordered phase. However, for lack of *in situ* characterization, the exact sites of Si and C atoms in a primitive cell cannot be definitely determined, so it is difficult to associate the long-range order with individual atoms of a particular species.

Finally, we emphasize that this Letter is suggestive for the synthesis of the $\text{Si}_{1-x}\text{C}_x$ alloy with high carbon concentration that is inaccessible by conventional routes. Furthermore, the superstructure identified in the material indicates that a new ordered phase has been observed in the pure Si-C system. Physical properties depend strongly on the composition and structure, which means that novel optical or electrical functions may be explored in the $\text{Si}_{1-x}\text{C}_x$ alloy.

This work was financially supported by the National Natural Science Foundation (Grant No. 10274082) and the

State Key Project of Fundamental Research (Grant No. 1998061309) of China. The authors would like to thank Professor Lin Cao, Professor Keming Fang, and Dr. Wenshen Hua for their help in the HRTEM experiments.

-
- [1] I. N. Remediakis, E. Kaxiras, and P. C. Kelires, *Phys. Rev. Lett.* **86**, 4556 (2001).
 - [2] P. Sonnet, L. Stauffer, A. Selloni, A. D. Vita, R. Car, L. Simon, M. Stoffel, and L. Kubler, *Phys. Rev. B* **62**, 6881 (2000).
 - [3] J. Kouvetakis, D. Chandrasekhar, and D. J. Smith, *Appl. Phys. Lett.* **72**, 930 (1998).
 - [4] D. Chandrasekhar, J. McMurran, D. J. Smith, J. Kouvetakis, J. D. Lorentzen, and J. Menéndez, *Appl. Phys. Lett.* **72**, 2117 (1998).
 - [5] A. Ourmazd and J. C. Bean, *Phys. Rev. Lett.* **55**, 765 (1985).
 - [6] J. L. Martins and A. Zunger, *Phys. Rev. Lett.* **56**, 1400 (1986).
 - [7] P. B. Littlewood, *Phys. Rev. B* **34**, 1363 (1986).
 - [8] S. Ciraci and I. P. Batra, *Phys. Rev. B* **38**, 1835 (1988).
 - [9] F. K. LeGoues, V. P. Kesan, and S. S. Iyer, *Phys. Rev. Lett.* **64**, 40 (1990).
 - [10] F. K. LeGoues, V. P. Kesan, S. S. Iyer, J. Tersoff, and R. Tromp, *Phys. Rev. Lett.* **64**, 2038 (1990).
 - [11] V. P. Kesan, F. K. LeGoues, and S. S. Iyer, *Phys. Rev. B* **46**, 1576 (1992).
 - [12] A. D. Pino, Jr., A. M. Rappe, and J. D. Joannopoulos, *Phys. Rev. B* **47**, 12 554 (1993).
 - [13] J. Tersoff, *Phys. Rev. Lett.* **64**, 1757 (1990).
 - [14] H. Dai, A. G. Rinzler, P. Nikolaev, A. Thess, D. T. Colbert, and R. E. Smalley, *Chem. Phys. Lett.* **260**, 471 (1996).
 - [15] R. O. Jones, *J. Chem. Phys.* **110**, 5189 (1999).
 - [16] F. Tsui and P. A. Ryan, *Phys. Rev. Lett.* **89**, 015503 (2002).
 - [17] J. Tersoff, *Phys. Rev. Lett.* **74**, 5080 (1995).
 - [18] W. Kim, H. Kim, G. Lee, and J. Koo, *Phys. Rev. Lett.* **89**, 106102 (2002).
 - [19] P. C. Kelires and E. Kaxiras, *Phys. Rev. Lett.* **78**, 3479 (1997).
 - [20] H. Rücker, M. Methfessel, E. Bugiel, and H. J. Osten, *Phys. Rev. Lett.* **72**, 3578 (1994).
 - [21] P. J. Bedrossian, *Surf. Sci.* **320**, 247 (1994).
 - [22] P. J. Bedrossian, *Surf. Sci.* **322**, 73 (1995).